Supporting Information

Raman spectroscopic evidence of the *pseudo*-rotational isomerization of *N*-alkyl-*N*-methylpyrrolidinium bis-(trifluoromethanesulfonyl) amide ionic liquids

Yasuhiro Umebayashi [†,*] Takushi Mistugi [†], Kenta Fujii [&], Shiro Seki [‡], Kazumi Chiba [#], Hideo Yamamoto [#], José N. Canongia Lopes [$,*], Agílio A. H. Pádua [§,*], Munetaka Takeuchi [†], Ryo Kanzaki [†] and Shin-ichi Ishiguro[†]

[†] Department of Chemistry, Faculty of Science, Kyushu University
Hakozaki, Higashi-ku, Fukuoka, 8128-8581, Japan
[‡] Materials Science Research Laboratory, Central Research Institute of Electric Power Industry (CRIEPI), 2-11-1, Iwado-kita, Komae, Tokyo 201-8511, Japan,
[&] Department of Chemistry and Applied Chemistry, Faculty of Science and Engineering, Saga University, Honjo-machi, Saga 840-8502, Japan
[#] Japan Carlit Co. Ltd., 2470 Handa, Sibukawa-Shi, Gunma, 377-0004, Japan
[$] Centro de Química Estrutural, Instituto Superior Técnico, 1049 001 Lisboa, and Instituto de Tecnologia Química e Biológica, UNL, Av. República Ap. 127, 2780 901 Oeiras, Portugal
[§]Laboratoire Thermodynamique et Interactions Moléculaires, Université Blaise Pascal Clermont-Ferrand/CNRS FRE3099, France

[*] Corresponding author: yumescc@mbox.nc.kyushu-u.ac.jp (YU), jnlopes@ist.utl.pt (JNCL) and agilio.padua@univ-bpclermont.fr (AAHP)

Figure S1

Raman spectra for $[P_{13}]$[TFSA] in the frequency range 200-1700 cm^{-1} at 298 K and theoretical Raman spectra at the optimized geometries at the B3LYP/6-311+G(d,p) level of theory..

Figure S2

Raman spectra for $[P_{14}]$[TFSA] in the frequency range 200-1700 cm^{-1} at 298 K and theoretical Raman spectra at the optimized geometries at the B3LYP/6-311+G(d,p) level of theory..

Figure S3

Typical curve fitting results of the observed Raman spectra and the corresponding theoretical ones for $[P_{13}]$[TFSA] at the frequency range 870-960 cm^{-1} (*a*) and for $[P_{14}]$[TFSA] at 860-950 cm^{-1} (*b*).

Figure S4

Typical curve fitting results for the observed Raman spectra and the corresponding theoretical ones for $[P_{13}]$[TFSA] (*a*) and for $[P_{14}]$[TFSA] (*b*) at the frequency range 350-470 cm^{-1}.

Figure S5

Distribution of the CS··SC dihedral angle in $TFSA^{-}$ found in the CSD database for non coordinated (*a*) and metal coordinated $TFSA^{-}$ (*b*), respectively.

Figure S6

Dihedral angle distributions of C2-C3-C4-C5 (*a*) and C3-C2-N1-C7 (*b*) for $[P_{13}]$[TFSA] and those for $[P_{14}]$[TFSA], respectively. Panel (*c*) and (*d*) are corresponding to the panel (*a*) and (*b*).

Figure S7

Dihedral of the CS··SC angle distributions in $TFSA^{-}$ for $[P_{13}]$[TFSA] (*a*) and for $[P_{14}]$[TFSA] (*b*), respectively.

Figure S1

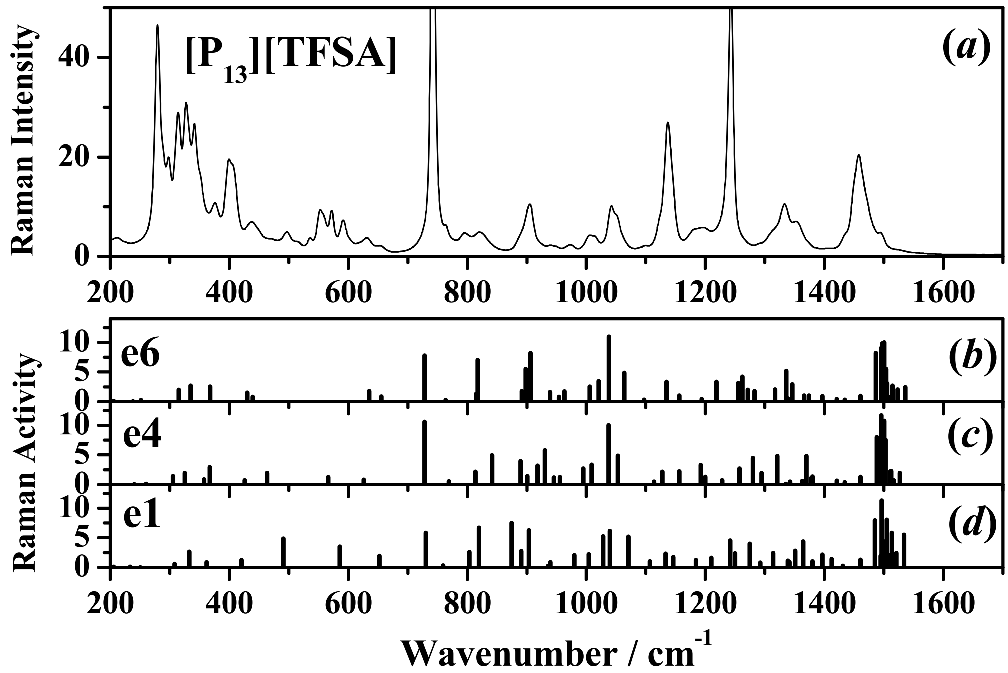

[P13][TFSA]
(a)
(b)
(c)
(d)
e6
e4
e1
Raman Intensity
Raman Activity
Wavenumber / cm-1
0
20
40
0
5
10
200
400
600
800
1000
1200
1400
1600

Figure S2

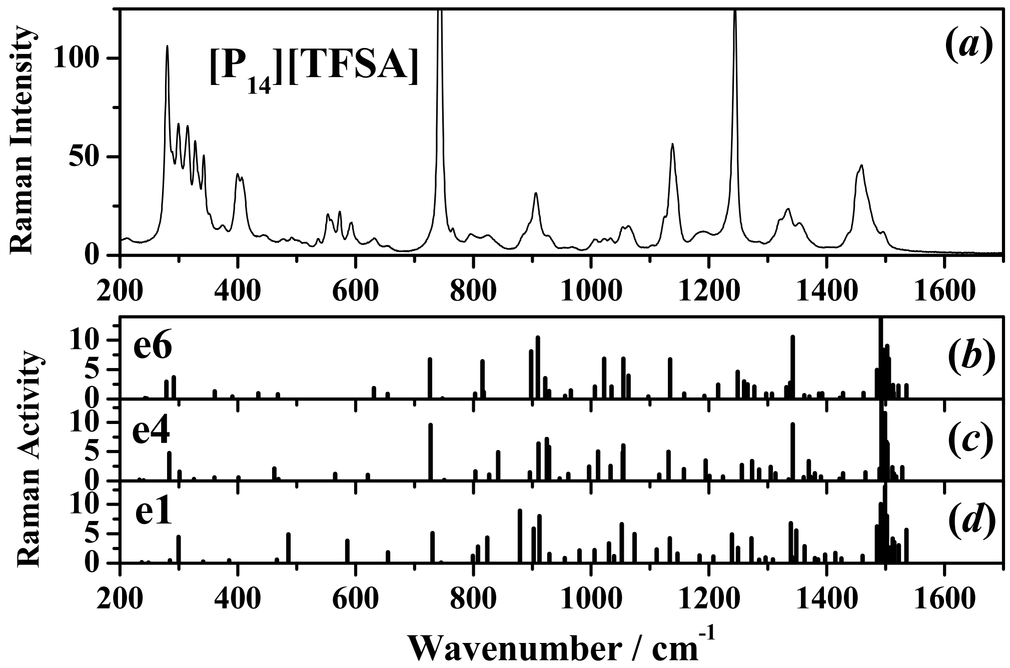

Raman Intensity
[P14][TFSA]
(a)
100
50
0
200
400
600
800
1000
1200
1400
1600
Raman Activity
e6
(b)
e4
(c)
e1
(d)
10
5
0
Wavenumber / cm-1

Figure S3

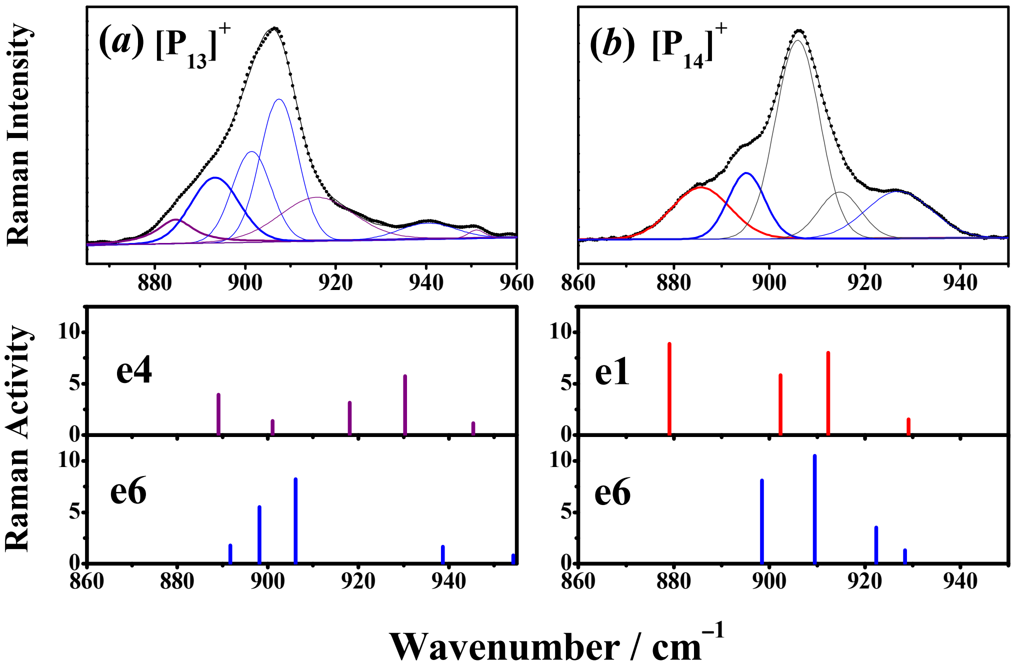

(a) [P13]+
(b) [P14]+
Raman Intensity
Raman Activity
e4
e6
e1
e6
880
900
920
940
960
860
10
5
0
Wavenumber / cm-1

Figure S4

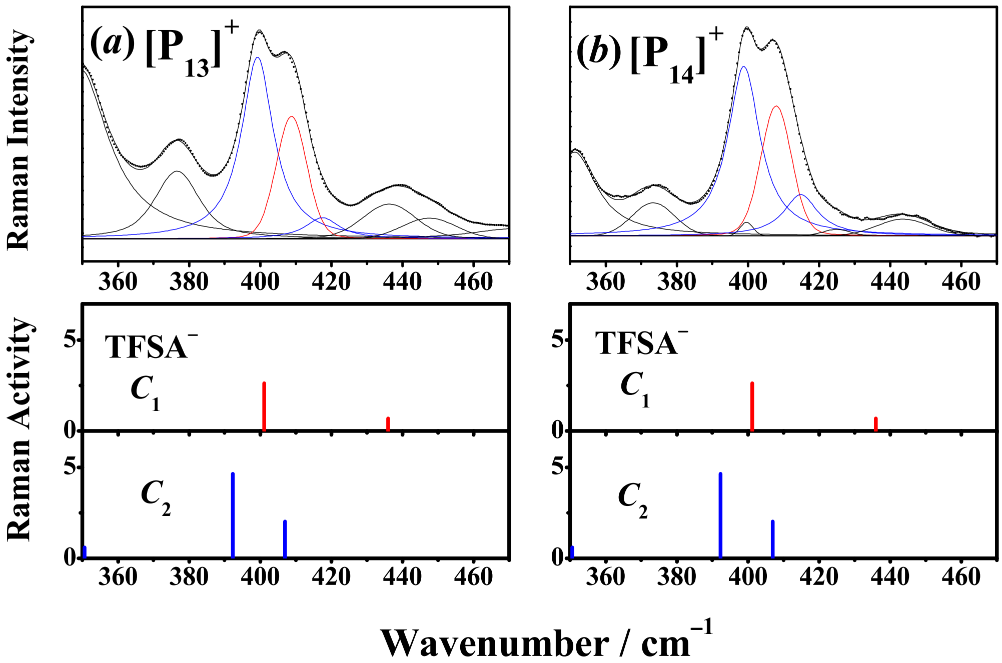

(a) [P13]+
(b) [P14]+
Raman Intensity
Raman Activity
TFSA−
C1
C2
0
5
360
380
400
420
440
460
Wavenumber / cm−1

Figure S5

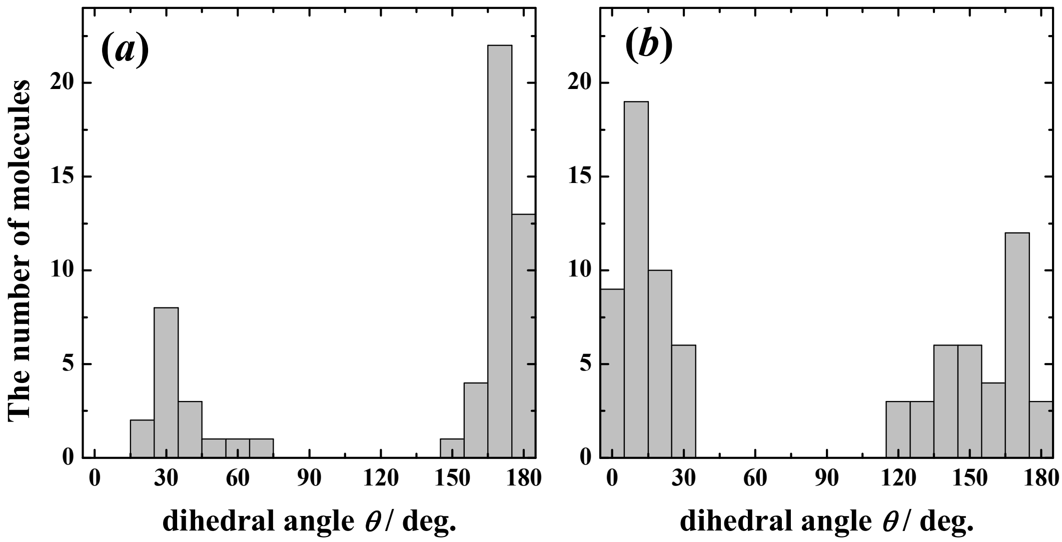

(a)
(b)
The number of molecules
0
5
10
15
20
0
30
60
90
120
150
180
dihedral angle θ / deg.
dihedral angle θ / deg.

Figure S6

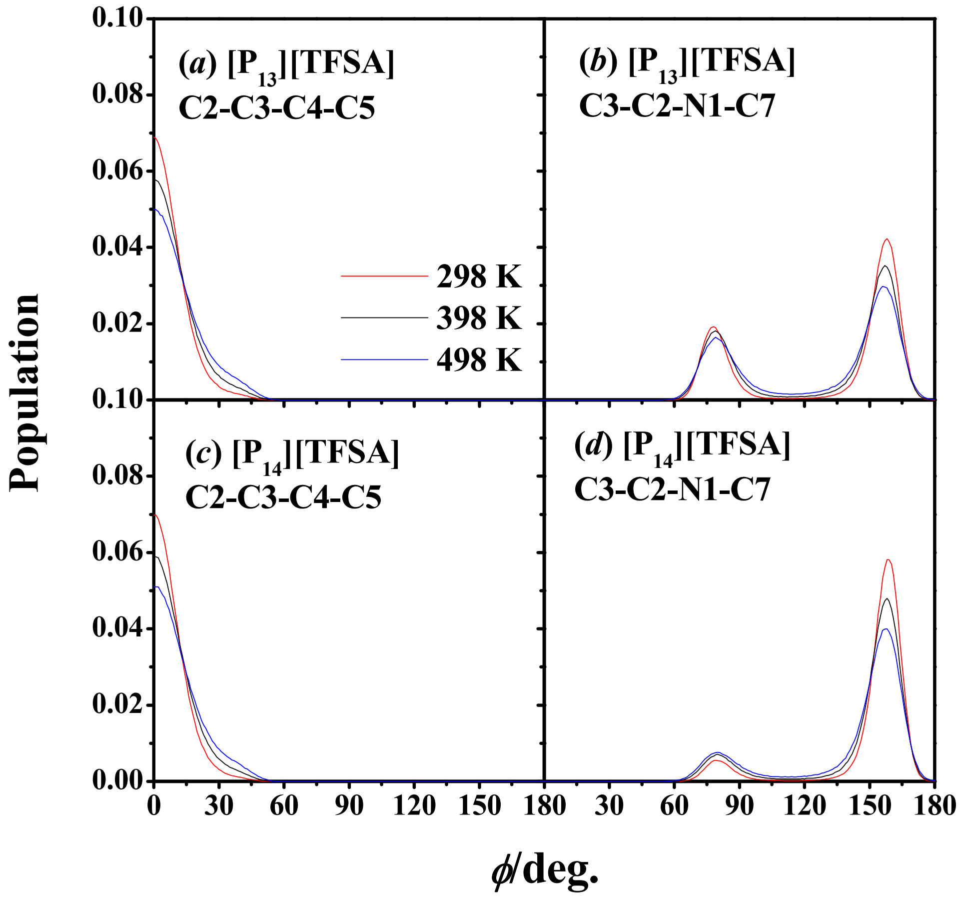

(a) [P13][TFSA]
C2-C3-C4-C5
(b) [P13][TFSA]
C3-C2-N1-C7
(c) [P14][TFSA]
C2-C3-C4-C5
(d) [P14][TFSA]
C3-C2-N1-C7
298 K
398 K
498 K
Population
ϕ/deg.

Figure S7

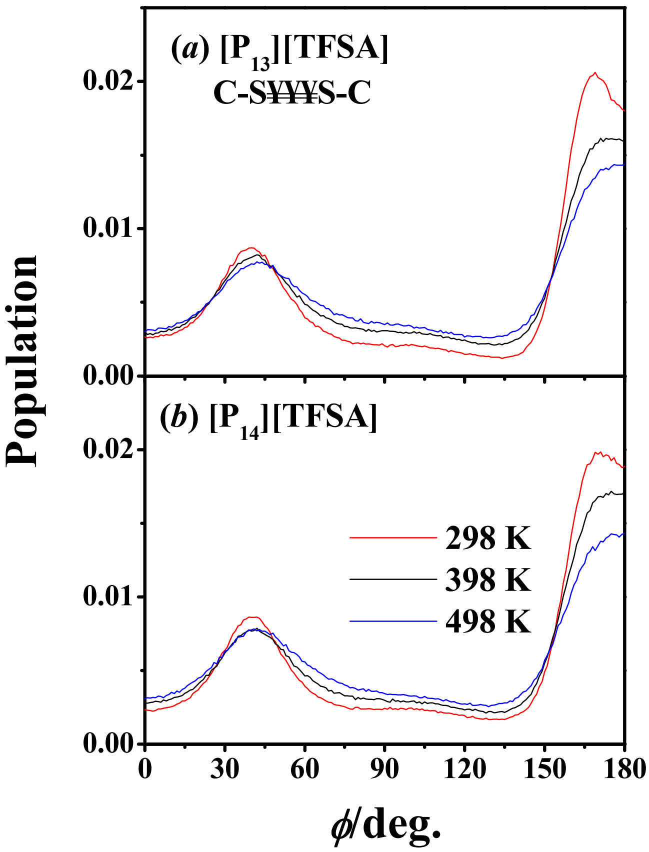

(a) [P13][TFSA]
C-S¥¥¥S-C
0.02
0.01
0.00
Population
(b) [P14][TFSA]
298 K
398 K
498 K
0
30
60
90
120
150
180
φ/deg.

Table S1 Structural parameters, bond length / Å, bond angles / deg. and dihedral angles / deg, and the energy corrected with zero point energy ΔE_{ZPE} / kJ mol^{-1}, thermodynamic parameters, Gibbs free energy $\Delta G°$ / kJ mol^{-1} and enthalpy $\Delta H°$ from the e6 to the other isomers and dipole moment μ / Debye at the optimized geometries calculated at the B3LYP/6-311+G(d,p) level of theory. The experimental enthalpies for the isomerization from the e6 to the e1 for $[P_{14}]^+$ and to the e4 for $[P_{13}]^+$ cations evaluated by Raman measurement with varying temperature are also listed.

	P_{13}^+			P_{14}^+		
	e1	e4	e6	e1	e4	e6
Bond Lengths						
N1–C2	1.523	1.548	1.524	1.523	1.548	1.524
N1–C5	1.527	1.538	1.526	1.526	1.537	1.526
N1–C6	1.499	1.504	1.505	1.499	1.504	1.504
N1–C7	1.532	1.527	1.523	1.533	1.527	1.524
C2–C3	1.531	1.531	1.534	1.531	1.532	1.534
C3–C4	1.555	1.534	1.555	1.555	1.534	1.554
C4–C5	1.535	1.521	1.534	1.535	1.521	1.533
C7–C8	1.527	1.526	1.527	1.526	1.525	1.526
C8–C9	1.536	1.535	1.535	1.540	1.539	1.539
C9–C10				1.531	1.531	1.531
Bond angles						
C2–N1–C5	101.9	105.1	102.4	101.9	105.1	102.5
C2–N1–C6	111.7	110.2	110.6	111.2	110.3	110.5
C2–N1–C7	112.2	112.1	112.8	109.0	112.0	112.8
C5–N1–C6	111.2	109.2	109.7	111.7	109.2	109.7
C5–N1–C7	108.9	109.3	110.3	112.2	109.5	110.3
C6–N1–C7	110.6	110.7	110.8	110.6	110.7	110.8
N1–C2–C3	105.3	106.3	105.4	105.3	106.3	105.5
C2–C3–C4	105.4	103.8	105.6	105.3	103.9	105.7
C3–C4–C5	105.4	102.2	105.5	105.4	102.3	105.5
N1–C5–C4	105.6	105.2	105.7	105.6	105.2	105.7
N1–C7–C8	116.4	115.9	115.8	116.4	115.8	115.8
C7–C8–C9	109.9	110.2	110.2	110.3	110.6	110.4
C8–C9–C10				112.4	112.4	112.4
Dihedral Angles						
C5–N1–C2–C3	−39.8	−2.8	38.1	−39.6	−1.9	37.7
C6–N1–C2–C3	−158.6	−120.4	−78.7	−158.5	−119.5	−79.1
C7–N1–C2–C3	76.6	115.8	156.7	76.8	116.8	156.2
C2–N1–C5–C4	38.0	−22.6	−37.7	38.1	−23.4	−37.6
C6–N1–C5–C4	157.2	95.4	79.8	157.3	94.9	79.8
C7–N1–C5–C4	−80.8	−143.4	−157.9	−80.6	−143.8	−157.9
C2–N1–C7–C8	64.4	69.6	64.3	65.3	69.5	64.2
C5–N1–C7–C8	176.5	−174.3	178.1	177.5	−174.3	178.0
C6–N1–C7–C8	−60.4	−53.9	-60.3	−60.0	−54.0	−60.3
N1–C2–C3–C4	26.4	26.94	−24.3	26.1	26.1	−23.8
C2–C3–C4–C5	-2.1	-40.7c	0.9	−22.3	−40.3	0.3
C3–C4–C5–N1	−22.0	39.4	22.8	−22.3	39.5	23.0
N1–C7–C8–C9	−179.1	−174.1	−176.8	−178.7	−173.7	−175.8
C7–C8–C9–C10				−179.2	−178.5	−179.2
ΔE_{ZRE}/kJmol^{-1}	3.69	3.36	0.00	2.78	2.41	0.00
$\Delta G°$/kJmol^{-1}	2.12	1.53	0.00	2.24	1.98	0.00
$\Delta H°$/kJmol^{-1}	0.36	1.63	0.00	2.38	3.34	0.00
Dipole moment/*D*	2.18	1.65	1.55	3.80	3.47	3.39

Table S2 Raman spectroscopic data for [P_{13}][TFSA] and [P_{14}][TFSA] ionic liquids recorded at 298 K and normal mode frequencies, Raman activities and IR intensities calculated at the optimized geometries for the *pseudo*-rotational isomers of [P_{13}] and [P_{14}] ions based on the B3LYP/6-311+G(d,p) level of theory.

		$P_{13}^{+}TFSA^{-}$								
$TFSA^{-}$	P_{13}^{+}	e1			e4			e6		
obs/cm^{-1}	obs/cm^{-1}	freq/cm^{-1}	Raman	IR	freq/cm^{-1}	Raman	IR	freq/cm^{-1}	Raman	IR
209.5, VW		35.67	0.1	0.1	40.40	0.2	0.5	77.28	0.1	0.0
280, S		79.38	0.4	0.2	86.46	0.2	0.1	100.14	0.2	0.7
289, M(sh)		118.62	0.3	0.2	131.04	0.1	0.3	104.15	0.1	0.1
297.5, M		186.74	0.2	0.2	173.08	0.2	0.2	148.27	0.1	0.6
314.5, M		204.88	0.1	0.1	240.04	0.0	0.1	205.38	0.1	0.3
328, M		232.67	0.1	0.0	260.03	0.1	0.3	237.82	0.0	0.0
333, M(sh)		250.20	0.0	0.1	305.36	1.4	0.0	251.15	0.2	0.1
342.5,		308.28	0.6	0.1	325.41	1.9	0.1	314.61	2.0	0.1
351.5, W		332.52	2.7	0.1	357.64	0.9	0.2	334.69	2.7	0.1
	374.5, W e6	362.11	0.8	0.2	366.88	2.9	0.2	367.51	2.5	0.3
399, M	438, W e6	420.25	1.2	0.6	425.65	0.7	0.4	429.80	1.4	0.5
408, M	449,							439.53	0.9	0.3
513, VW	469, VW e4				463.42	2.0	0.4			
536, VW	497.5, VW	490.82	4.9	0.1	566.19	1.2	1.8			
553, W		584.70	3.5	3.7	625.81	0.8	0.8	635.43	1.8	1.5
557.5,	652.5, VW	652.66	1.9	0.5	727.93	10.6	2.1	654.74	0.9	0.2
572, W		729.74	5.9	2.1	768.77	0.5	5.1	728.04	7.7	2.1
591.5, W		759.07	0.3	5.5	813.38	2.1	9.1	763.35	0.2	4.6
601,		802.99	2.7	3.0	841.57	4.9	8.6	815.29	1.0	4.7
631.5, VW	820, W e6	820.02	6.6	3.5				817.05	7.3	4.8
742, VS	889, W(sh)	874.18	7.5	26.3	889.10	3.9	7.6	891.35	1.7	1.8
763, W	899, W(sh)	890.76	2.8	1.6				898.12	5.6	1.0
796, W	906.5, W e6	903.29	6.3	6.0	901.00	1.4	4.4	906.13	8.1	12.5
	916.5,	935.54	0.3	11.0	918.09	3.2	1.4	938.69	1.6	21.6
	940, VW e4	939.86	0.9	6.8	930.31	5.7	9.2			
	949, VW e4				945.35	1.2	15.3	954.18	0.8	4.4
	973, VW e6	979.60	2.1	2.4	955.88	1.3	20.7	962.98	1.7	23.0
	1005, VW	1004.10	2.2	9.3	995.14	2.7	12.2	1005.45	2.6	9.1
	1013.5, VW	1027.93	5.2	7.8	1008.70	3.3	7.0	1020.69	3.4	4.1
	1042, W(sh)	1039.36	6.2	9.8	1053.02	4.9	1.7			
	1048, W e6							1037.80	11.0	8.7
	1063.5,	1070.48	5.2	7.1	1113.78	0.5	2.0	1063.54	4.8	1.5
	1100, VW	1106.58	1.0	0.5	1127.70	2.2	0.6	1097.00	0.3	0.5
		1132.99	2.3	1.0	1156.11	2.2	1.0	1135.01	3.3	2.6
		1146.09	1.7	0.2	1192.56	3.3	1.4	1156.30	1.0	0.9
		1184.16	1.2	0.2	1200.04	1.3	0.7	1194.06	0.4	0.0
1125, W(sh)		1210.27	1.6	0.5	1228.09	0.7	3.4	1218.56	3.4	0.2
1137, M	1261,	1241.41	4.5	2.2	1257.50	2.7	2.7	1255.49	3.1	3.6
1190, W(br)		1249.96	2.4	0.8				1262.38	4.2	0.2
1243, S		1274.68	4.0	5.8	1280.16	4.5	0.9	1271.11	2.0	3.4
	1292.5, VW	1292.47	0.8	2.6	1294.52	2.0	3.4	1283.12	1.8	3.4
	1313, W(sh)	1314.03	2.5	0.5	1321.13	4.8	1.3	1316.73	2.1	0.8
		1338.89	1.1	0.1	1335.49	0.1	2.1	1336.22	5.3	1.6
		1341.18	0.9	1.6	1342.35	0.5	0.5	1338.96	0.5	1.1
	1352.5 W e1	1351.21	2.7	3.7	1362.76	0.6	0.2	1346.09	2.8	0.6
1333, W	1369,	1364.09	4.4	1.7	1370.05	4.8	8.7	1366.29	1.0	3.5
		1380.29	1.0	3.5	1378.17	1.1	2.9	1374.07	1.0	3.7
		1396.99	2.1	0.7	1380.04	1.3	1.5	1396.56	0.9	5.8
	1439, W(sh)	1412.77	1.5	1.1	1420.95	0.6	2.0	1421.42	0.4	2.0
	1452, M(sh)	1431.40	0.3	3.0	1434.37	0.4	3.5	1434.56	0.3	4.0

1458, M e6	1460.61	1.3	3.3	1461.16	1.3	8.3	1460.85	1.0	10.7
1467.5,	1485.46	7.8	0.4	1488.48	8.0	3.4	1486.40	8.2	1.7
1484, W(sh)	1494.76	2.2	3.0	1495.84	11.7	2.8	1495.64	9.0	3.4
1494, W(sh)	1495.72	10.7	3.7	1498.71	5.6	11.7	1497.41	9.9	1.3
	1497.73	3.3	15.2	1499.99	3.9	24.1	1500.55	9.8	10.9
	1503.81	4.5	18.4	1500.72	10.7	3.7	1503.77	5.5	11.4
	1505.01	7.9	3.9	1503.04	7.6	13.6	1505.53	3.2	17.6
	1510.06	2.1	15.1	1510.75	2.2	6.6	1512.14	0.8	17.4
	1513.39	6.0	12.1	1512.45	2.2	16.9	1514.24	2.7	1.4
	1520.95	2.3	37.1	1516.64	0.7	13.4	1522.98	2.0	33.4
	1533.50	5.5	7.9	1526.97	2.0	3.9	1536.29	2.4	2.5
	3037.77	173.2	6.8	3036.59	219.1	1.0	3037.63	203.3	3.8
	3047.59	39.9	14.5	3040.44	9.6	21.1	3043.13	26.8	18.1
	3071.57	63.8	0.5	3056.55	139.1	1.7	3061.91	28.3	8.3
	3072.97	27.9	7.3	3059.24	54.2	8.6	3075.09	72.1	0.3
	3078.11	39.3	7.0	3064.14	24.6	12.4	3079.50	32.9	7.2
	3080.62	68.3	0.6	3071.04	84.1	0.5	3080.02	42.6	2.1
	3083.43	14.3	1.9	3076.12	110.9	2.2	3082.75	10.4	0.5
	3086.47	117.9	9.1	3087.24	76.4	4.9	3085.72	50.4	13.7
	3088.72	279.5	4.2	3101.01	59.5	3.2	3088.26	358.3	0.9
	3105.47	14.7	19.4	3101.40	12.7	10.0	3102.84	9.9	11.3
	3113.76	35.3	0.8	3114.57	26.6	18.3	3113.33	31.3	0.5
	3119.73	87.9	9.1	3117.65	162.7	1.0	3117.77	21.7	18.1
	3127.77	82.7	5.4	3119.37	89.3	10.2	3119.54	84.0	10.6
	3132.65	43.9	10.9	3122.34	64.5	5.5	3128.63	106.8	3.2
	3144.76	36.3	4.1	3146.71	42.4	3.3	3144.89	39.2	3.8
	3157.42	38.3	2.0	3157.92	42.4	2.0	3152.99	37.3	3.5
	3159.60	49.5	3.4	3161.83	29.0	3.7	3167.08	41.2	1.6
	3173.10	37.2	1.5	3172.96	34.4	1.0	3178.65	31.9	1.4
Scaling				0.9993					

Table S2 *Continued*

		$P_{14}^{+}TFSA^{-}$								
$TFSA^{-}$	P_{14}^{+}	e1			e4			e6		
obs/cm^{-1}	obs/cm^{-1}	freq/cm^{-1}	Raman	IR	freq/cm^{-1}	Raman	IR	freq/cm^{-1}	Raman	IR
209.5 VW		38.76	0.2	0.2	44.86	0.2	0.5	56.81	0.1	0.3
280.5 S		67.73	0.4	0.2	69.06	0.2	0.3	68.53	0.1	0.2
289.0 M		102.87	0.2	0.1	82.43	0.1	0.1	83.24	0.1	0.1
299.0 M		109.65	0.1	0.2	123.03	0.0	0.1	108.14	0.1	0.4
314.5 M		149.71	0.1	0.1	170.11	0.0	0.4	134.57	0.0	0.4
328.0 M		196.98	0.3	0.2	233.40	0.2	0.3	189.95	0.1	0.5
334.0 M(sh)		237.27	0.2	0.0	240.03	0.1	0.1	243.03	0.1	0.1
342.5 M		248.54	0.1	0.1	283.97	4.7	0.2	245.83	0.1	0.0
351.5 W		284.57	0.4	0.2	301.09	1.6	0.3	279.20	3.0	0.3
		299.55	4.5	0.4	325.63	0.3	0.1	291.50	3.6	0.2
	374.5 W, e6	341.10	0.3	0.2	360.49	0.6	0.2	360.72	1.3	0.2
399.0 M		385.40	0.5	0.1	401.50	0.6	0.1	391.27	0.4	0.1
408.0 M	445.0 VW(br), e6	466.65	0.6	0.6	462.21	2.1	0.4	434.85	1.0	0.3
501.0 W(sh)	477.5 VW, e6				469.12	0.3	0.5	468.16	0.8	0.7
517.0 W	492.0 VW, e1	485.99	4.9	0.1						
537.0 W	632.0 W, e6	586.23	3.8	4.0	565.60	1.2	1.8	631.41	1.8	1.6
553.0 M	655 W, e6	654.81	1.8	0.5	620.86	1.0	0.9	654.27	0.9	0.1
558.5 M		730.32	5.1	2.5	727.48	9.5	2.3	726.48	6.7	2.3
573.0 M		745.21	0.1	4.7	750.61	0.2	3.7	747.40	0.1	4.3
593.0 M		799.31	1.3	2.2	803.33	1.6	5.9	802.78	0.9	1.6
601.5 W(sh)		808.06	2.8	1.7	826.82	1.1	5.1	815.86	6.7	4.5
743.0 VS	824.0 W, e1	822.95	4.4	4.0				817.48	0.9	4.8
765.0 W	843.0 W(sh), e4				842.16	4.9	9.0			
795.0 W	886.0 VW(sh), e1	879.07	8.9	36.3	895.58	1.5	13.1			
	895.0 W(sh), e6							898.48	8.1	1.7
	906.0 M, e6							909.53	10.5	1.1
	925.5 M, e6	902.28	5.8	9.2	910.49	6.4	1.3	922.36	3.6	39.9
		912.35	8.0	2.5	924.67	7.2	2.2	928.40	1.3	9.8
	955.5 VW, e6	929.08	1.6	4.1	928.68	5.8	34.4	955.86	0.5	2.5
	968.5 VW, e6	955.21	0.8	2.8	946.84	0.5	2.5	965.47	1.4	5.9
	1007.5 W, e6	980.29	2.1	1.2	961.13	1.2	4.0	1006.32	2.1	9.0
	1022.0 W, e6	1005.67	2.2	7.3	996.29	2.4	12.3	1022.15	6.9	8.4
	1033.0 W, e6	1030.03	3.4	8.0	1011.8	5.0	5.2	1034.35	2.1	5.3
	1053.5 W, e6	1039.16	1.2	7.3	1033.21	2.5	7.0	1054.43	6.8	5.8
	1063.5 W, e6	1052.08	6.6	5.0	1053.78	4.8	1.6	1063.43	4.0	0.9
		1073.57	4.9	6.9	1054.47	6.1	5.8			
	1105.0 VW, e1	1111.46	2.3	2.3	1115.7	1.1	3.5	1096.98	0.4	0.5
1125.0 W		1133.65	4.2	2.7	1131.13	5.0	2.4	1133.98	6.7	6.7
1138.0 M		1146.73	1.6	0.3	1157.52	2.1	1.6	1158.01	0.9	0.9
1190.0 W(br)		1183.97	1.3	0.7	1194.29	3.5	1.5	1192.42	0.5	0.0
		1207.57	1.1	0.9	1200.85	0.9	0.8	1215.87	2.4	0.4
	1229.0 M(sh), e1	1239.19	4.9	1.2	1223.94	0.8	3.5	1249.01	4.6	2.0
1244.0 VS		1249.24	2.6	1.7	1255.93	2.7	2.9	1259.56	3.0	0.4
	1261.0 VW(sh), e6	1271.80	4.2	4.4	1273.18	3.4	1.3	1265.39	2.5	2.2
		1285.32	0.6	2.0	1285.25	2.0	0.4	1277.52	2.1	4.6
	1291.0 VW, e6							1296.95	0.9	2.3
	1308.0 VW(sh), e4	1296.08	0.9	3.9	1305.01	2.4	1.6			
		1308.44	0.7	0.9	1312.81	1.3	4.4	1306.99	0.9	1.0
	1322.0 M, e6	1338.80	6.8	1.4	1335.22	0.3	2.4	1331.53	2.0	1.7
1334.5 M		1340.85	1.0	0.7	1342.29	9.7	0.9	1337.63	2.6	1.5
		1348.10	5.6	3.7	1360.98	0.6	0.2	1342.24	10.7	1.5
	1352.5 M, e6							1362.05	0.6	3.0
	1368.0 VW(sh), e4	1362.22	2.9	0.7	1369.14	3.4	5.8			

	1379.87	0.9	3.0	1372.67	0.7	2.6	1370.46	0.4	2.2
	1385.23	0.7	5.7	1379.85	1.3	1.3	1386.53	0.9	3.2
	1396.89	1.4	0.5	1389.81	0.8	6.9	1392.26	1.0	9.9
	1414.53	1.7	4.9	1421.66	0.4	6.0	1422.15	0.2	5.6
	1424.96	0.8	1.9	1427.75	1.3	2.8	1427.57	1.0	2.7
1437.0 W(sh), e1	1460.64	1.2	3.5	1465.84	1.4	7.2	1462.08	1.0	9.9
1452.0 S(sh), e6	1485.55	6.2	0.8	1489.53	2.1	3.2	1485.19	4.8	1.7
1459.0 S, e6	1491.85	9.9	1.8	1492.99	18.1	2.4	1491.70	18.5	1.6
1470.0 S(sh), e6	1496.89	4.0	8.9	1497.3	8.8	7.8	1496.43	8.5	2.9
1482.0 M(sh), e6	1498.70	12.8	1.2	1499	11.6	2.5	1498.90	4.1	1.8
1497.0 M, e6	1499.98	1.0	10.7	1501.35	6.7	13.5	1502.13	2.3	5.2
	1502.02	8.0	14.1	1502.78	1.9	27.4	1502.78	9.2	15.6
	1506.96	2.7	9.8	1503.11	6.4	3.8	1505.54	6.6	23.9
	1511.74	4.0	8.7	1511.44	2.4	12.3	1512.67	2.6	6.2
	1514.40	3.7	15.3	1514.06	1.3	14.0	1513.15	0.8	3.2
	1521.98	3.0	36.6	1517.97	0.8	9.5	1521.56	2.3	35.5
	1535.39	5.7	8.0	1527.89	2.4	3.4	1535.37	2.3	2.8
	3017.65	148.7	10.4	3018.27	159.4	9.0	3017.86	153.6	10.1
	3030.91	48.5	10.5	3029.97	16.3	9.9	3030.78	40.2	11.0
	3035.33	110.9	26.5	3033.84	146.5	28.5	3035.05	126.6	26.8
	3045.56	95.8	4.5	3046.13	99.8	4.0	3045.62	103.3	3.7
	3070.96	55.4	0.5	3056.37	149.4	2.0	3060.37	34.1	9.2
	3072.55	13.1	8.5	3060.19	44.0	9.4	3074.54	7.8	4.4
	3078.34	18.7	10.6	3064.29	27.3	12.1	3077.95	31.8	7.4
	3078.90	38.5	2.4	3071.05	65.5	1.0	3081.62	16.4	1.9
	3083.74	20.9	2.3	3075.36	48.3	7.3	3083.00	13.2	1.1
	3086.23	124.6	7.7	3085.87	83.3	5.1	3084.65	89.7	13.2
	3089.14	270.3	4.9	3095.2	37.8	35.8	3088.51	325.9	1.9
	3095.36	38.4	39.9	3102.49	56.4	3.2	3095.30	38.9	35.7
	3109.23	100.3	16.7	3108.88	101.8	17.2	3108.93	103.3	17.1
	3113.77	34.7	0.8	3113.51	16.9	12.8	3112.11	31.5	0.9
	3127.72	85.5	5.4	3117.76	169.4	0.8	3114.10	9.7	14.7
	3132.53	45.4	9.0	3122.6	66.9	5.7	3127.63	110.5	3.2
	3145.46	36.0	4.0	3146.1	43.1	3.5	3144.43	39.4	3.7
	3158.15	43.1	2.0	3158.89	47.4	1.8	3152.43	35.0	3.5
	3160.61	44.4	3.5	3163.36	25.8	4.0	3169.97	42.2	1.5
	3172.05	35.8	1.6	3174.12	33.0	1.1	3181.49	29.8	1.7
Scaling Factor				1.006					

Table S3 Normal mode frequencies, Raman activities and IR intensities calculated at the optimized geometries for the $[P_{14}]^+$ e6 isomers with *gauche* butyl chains with respect to the C7-C8-C9-C10 dihedral angle based on the B3LYP/6-311+G(d,p) level of theory.

$[P_{14}]^+$					
60°			–60°		
Freq / cm^{-1}	Raman	IR	Freq / cm^{-1}	Raman	IR
37.83	0.2	0.1	38.23	0.1	0.2
75.31	0.2	0.5	82.95	0.1	0.6
98.82	0.1	0.1	106.71	0.1	0.1
126.62	0.2	0.8	124.85	0.2	0.8
139.54	0.0	0.5	145.54	0.1	0.4
194.10	0.1	0.5	202.56	0.1	0.3
226.63	0.5	0.1	226.10	0.8	0.3
258.65	0.1	0.2	258.72	0.1	0.2
284.75	2.0	0.1	281.04	2.0	0.1
332.22	1.0	0.2	334.71	1.0	0.2
365.93	3.0	0.3	367.55	1.7	0.3
401.19	0.8	0.3	415.03	2.3	0.2
429.91	1.5	0.6	436.21	0.8	0.5
451.89	0.5	0.2	442.67	0.7	0.3
635.78	1.7	1.7	636.32	1.7	2.0
654.96	0.9	0.2	655.56	1.0	0.3
726.59	7.3	2.9	725.24	6.7	1.9
758.31	0.4	4.7	763.42	1.0	4.8
793.14	0.9	2.4	800.36	0.8	2.3
816.62	5.5	3.0	814.31	1.7	4.7
818.21	2.5	7.3	817.62	6.9	5.7
884.09	8.1	0.5	880.53	7.1	0.3
900.34	13.8	1.0	900.57	14.6	0.8
922.16	2.4	43.2	920.80	3.5	39.0
926.74	2.2	4.5	931.72	1.2	7.2
956.75	0.7	9.2	955.19	0.7	2.9
970.60	1.0	0.4	969.17	2.2	14.0
1002.46	3.0	10.6	1008.03	1.1	8.8
1008.22	1.7	7.6	1009.12	2.2	4.9
1028.31	3.1	3.1	1027.46	4.7	3.8
1063.39	4.0	1.3	1063.63	5.2	2.0
1068.57	8.7	7.4	1067.66	6.1	5.2
1097.47	0.2	0.3	1097.15	0.2	0.5
1131.00	1.3	0.1	1133.90	1.6	0.7
1155.76	1.3	0.3	1150.88	1.4	3.1
1192.50	0.3	0.0	1191.62	0.1	0.2
1202.40	2.8	4.3	1209.71	3.1	0.6
1245.74	5.0	5.1	1248.11	3.5	1.5

1260.31	2.8	0.4	1261.19	2.2	1.7
1264.33	2.7	1.9	1266.35	4.0	2.9
1277.37	1.9	4.4	1276.62	2.7	4.7
1293.03	2.4	2.2	1297.68	1.2	1.4
1312.19	3.6	0.7	1309.25	4.1	3.9
1336.46	3.8	1.9	1334.99	4.8	2.0
1340.91	3.4	2.1	1340.20	0.3	0.7
1354.04	2.3	0.6	1355.44	3.9	0.0
1364.04	1.6	3.8	1366.24	1.0	2.7
1374.43	1.8	3.6	1373.15	3.9	7.8
1384.44	1.5	7.4	1382.61	0.9	5.6
1394.98	1.3	5.4	1400.04	1.7	5.5
1427.92	0.5	6.8	1425.89	0.6	7.2
1428.92	0.4	1.6	1428.97	0.6	2.0
1461.58	1.0	10.9	1461.98	1.0	9.4
1485.29	9.4	2.8	1485.85	7.0	2.2
1491.68	10.9	3.7	1492.33	13.8	2.8
1496.01	5.4	4.1	1496.42	6.2	6.8
1499.19	16.5	2.6	1499.86	18.8	2.3
1502.33	1.5	12.2	1502.58	0.4	10.3
1504.96	0.2	9.0	1505.97	0.3	8.7
1507.80	1.8	18.8	1508.01	1.1	18.8
1510.49	4.5	11.7	1510.79	3.3	10.6
1514.40	2.9	0.9	1514.34	2.9	2.7
1522.91	2.8	34.7	1523.50	2.2	35.1
1537.52	2.4	2.7	1536.76	2.0	2.0
3025.24	251.0	1.4	3025.43	220.3	3.0
3028.11	18.8	21.6	3029.15	17.4	26.1
3035.22	46.9	20.9	3035.77	84.2	14.1
3066.33	51.9	2.7	3066.19	40.0	4.5
3066.97	92.9	1.6	3066.80	109.2	0.9
3076.46	22.9	4.0	3074.89	47.4	7.0
3079.29	33.7	7.4	3079.41	29.5	8.4
3081.41	53.7	8.2	3081.26	15.1	2.3
3084.61	8.6	3.6	3083.19	10.7	2.1
3086.06	141.4	10.3	3086.12	82.8	13.2
3089.76	280.3	2.5	3088.73	339.4	2.0
3091.05	10.4	47.6	3091.72	11.9	48.2
3105.46	115.3	16.9	3106.15	112.2	16.6
3112.89	29.1	0.8	3113.60	30.0	0.6
3124.84	11.2	8.9	3122.11	8.3	8.6
3128.21	104.5	2.4	3128.79	110.8	3.0
3144.43	40.2	4.6	3144.67	39.3	4.2
3154.71	34.0	3.1	3154.15	36.1	3.2
3167.33	42.4	1.7	3168.71	40.5	1.7
3178.78	31.5	1.5	3180.02	30.8	1.5

Table S4 Selected structural parameters for $[P_{13}]^+$ or $[P_{14}]^+$ ions found in the CSD.

	$P_{13}^{+\,a}$			
	e6 (9)	e1 (4)	e7 (1)	e8 (1)
CSD Code	ACOLOU ACOLUA NATPOO QOPZUQ SEJQII	ACOMAH QOPZUQ SEJQII	ACOLUA	QOPZUQ
Bond Lengths				
N1 - C2	1.503	1.507	1.457	1.530
C2 - C3	1.510	1.520	1.506	1.443
C3 - C4	1.542	1.544	1.535	1.510
C4 - C5	1.516	1.517	1.492	1.441
C5 - N1	1.501	1.515	1.477	1.538
N1 - C6	1.493	1.499	1.469	1.464
N1 - C7	1.505	1.519	1.521	1.481
C7 - C8	1.501	1.503	1.503	1.497
C8 - C9	1.519	1.536	1.477	1.519
C9 - C10				
Bond Angles				
N1 - C2 - C3	106.3	105.3	109.7	105.6
C2 - C3 - C4	104.3	104.7	103.4	104.1
C3 - C4 - C5	106.1	105.9	103.0	106.8
N1 - C5 - C4	104.3	104.4	113.2	107.8
C2 - N1 - C5	102.5	104.3	101.0	102.6
C2 - N1 - C6	110.2	110.9	126.4	113.4
C5 - N1 - C6	108.4	108.4	88.6	109.8
C6 - N1 - C7	112.5	111.4	112.2	110.7
C2 - N1 - C7	112.9	111.3	118.4	109.4
C5 - N1 - C7	109.0	110.2	97.8	110.7
N1 - C7 - C8	113.4	115.2	90.0	115.7
C7 - C8 - C9	108.8	108.7	89.6	111.7
C8 - C9 - C10				
Dihedral Angles				
N1 - C2 - C3- C4	-21.6	24.5	-31.5	-36.9
C2 - C3 - C4 - C5	-2.8	0.9	18.0	30.9
C3 - C4 - C5 - N1	26.1	-25.7	-0.1	-12.2
C4 - C5 - N1 - C2	-39.1	40.6	-18.3	-9.7
C5 - N1 - C2 - C3	38.0	-32.8	30.4	29.1

[a] WAWHIM contains disordered pyrroridinium ring.

	P_{14}^{+b}			
	e6 (11)	e7 (2)	e5 (1)	e10 (1)
CSD Code	LAZREK LEGJIR LEGJIR01 NEZBAW TECYAC TECTEG YEQVOG	LEGJIR LEGJIR01	YEQVOG	LEGJOX
Bond Lengths				
N1 - C2	1.485	1.442	1.520	1.472
C2 - C3	1.549	1.721	1.529	1.497
C3 - C4	1.533	1.622	1.620	1.516
C4 - C5	1.562	1.571	1.555	1.523
N1 - C5	1.499	1.470	1.514	1.522
N1 - C6	1.563	1.516	1.506	1.506
N1 - C7	1.512	1.644	1.561	1.531
C7 - C8	1.463	1.321	1.459	1.488
C8 - C9	1.572	1.609	1.460	1.522
C9 - C10	1.444	1.309	1.482	1.495
Bond Angles				
N1 - C2 - C3	100.4	92.8	101.4	108.3
C2 - C3 - C4	108.1	93.6	108.3	106.8
C3 - C4 - C5	102.3	105.2	97.6	105.0
N1 - C5 - C4	101.6	101.7	100.9	104.7
C2 - N1 - C5	104.2	105.5	101.9	104.0
C2 - N1 - C6	108.0	117.4	116.1	112.4
C5 - N1 - C6	105.4	110.3	109.1	110.4
C6 - N1 - C7	111.1	101.5	111.3	109.5
C2 - N1 - C7	112.0	106.9	112.7	113.8
C5 - N1 - C7	113.7	115.4	104.7	106.5
N1 - C7 - C8	111.2	121.7	102.9	118.6
C7 - C8 - C9	108.6	118.9	97.5	109.3
C8 - C9 - C10	112.1	110.5	105.5	110.4
Dihedral Angles				
N1 - C2- C3 - C4	-23.5	-54.5	-13.9	10.1
C2 - C3- C4 - C5	-4.0	31.2	-18.4	11.4
C3 - C4- C5 - N1	30.0	2.0	43.8	-27.9
C4 - C5- N1 - C3	-47.3	-43.8	-56.2	34.1
C5 - N1 - C2 - C3	43.7	63.0	42.2	-27.4

[b] LEGJOX, NEYZUN and TECYIK include the butyl chain disordered structure, and SEJQOO, TECXUV and TECYIK contain the ring disorder.